WORLD CONFERENCE ON TIMBER ENGINEERING 2025
BRISBANE, AUSTRALIA

Advancing Timber for the Future Built Environment

A SIMPLIFIED APPROACH FOR ESTIMATING IN-PLANE LATERAL RESPONSE OF TIMBER-FRAMED PARTITION WALLS

Jitendra Bhatta[1], Joshua Mulligan[2], Rajesh P. Dhakal[3], Timothy J. Sullivan[4]

ABSTRACT: This study scrutinizes and refines the theoretical formulations predicting ultimate strength, initial stiffness, and drifts corresponding to screw damage and plasterboard lining buckling of partition walls using experimental data from published research. It also quantifies associated load and drift thresholds at different damage levels of a multi-winged timber-framed partition wall. The wall was constructed to reflect common New Zealand building practices and subjected to unidirectional quasi-static lateral cyclic drift demands. The predicted in-plane bi-linear load vs. drift backbone curve, using the refined formulations, reasonably capture the experimental backbone curve of the tested specimen, validating the reliability of the simplified approach.

KEYWORDS: Timber-framed partitions, Full scale, Quasi-static cyclic test, Damage thresholds, Back-bone curve

1 – INTRODUCTION

During the 2010-2011 Canterbury earthquake sequence, partition walls, being drift-sensitive, suffered widespread damage, including screw failures, lining cracks, and detachment [1]. Along with cold-formed steel, timber has been a common framing material for partition walls in New Zealand [2].

A partition wall typically consists of gypsum plasterboard linings secured with nails, screws, or adhesives to internal frames, and finished with plastering, sanding, and painting [3], [4]. Although partition walls are not considered part of the structural system in the seismic design of timber light-frame buildings, shake table tests on full-scale buildings [5]-[7] have shown that gypsum wallboard partitions or gypsum wallboard installed on the interior surfaces of structural wood shear walls can significantly impact the seismic response of timber buildings [8].

Theoretically, the shear strength of a rigid partition wall (where "rigid" refers to all frame members and plasterboard being securely attached and assumed functioning as a single unit) is generally estimated based on the shear strength of the screws that connect the linings to the internal framing [9]. The type of frame and the spacing of framing members are generally not considered significant factors in the wall's bracing strength [10]. Observations indicate that screw failures primarily occur around the wall perimeter and at the top and bottom runners [11]-[13]. It is assumed that lateral forces acting on the top runner are transferred to the lining through the top screws and then to the bottom runner via the screws at the bottom boundary, as shown in Fig. 1.

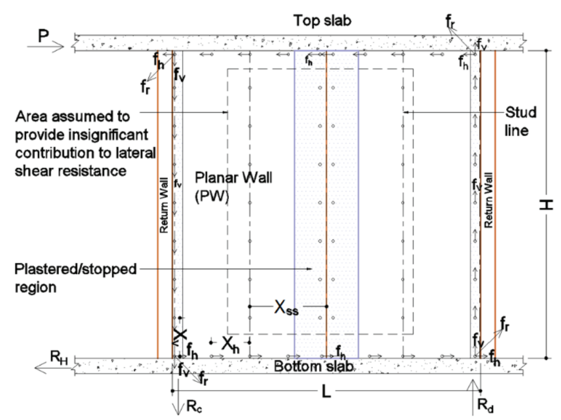

Figure 1. Schematic diagram of force transfer through a rigid partition wall [14]

[1] Jitendra Bhatta, Civil and Natural Resources Engineering, University of Canterbury, Christchurch, New Zealand jitendra.bhatta@canterbury.ac.nz

[2] Joshua Mulligan, BG&E, Christchurch, New Zealand, joshua.mulligan@bgeeng.com

[3] Rajesh P. Dhakal, Civil and Natural Resources Engineering, University of Canterbury, Christchurch, New Zealand rajesh.dhakal@canterbury.ac.nz

[4] Timothy J. Sullivan, Civil and Natural Resources Engineering, University of Canterbury, Christchurch, New Zealand timothy.sullivan@canterbury.ac.nz

https://doi.org/10.52202/080513-0688

The shear strength per unit length of the wall V_{fr}, with lining on both sides, corresponding to screw damage located at an extreme corner of the partition wall is given by (1) [9], [15].

$$V_{fr} = \frac{2f_r}{\lambda} \quad (1)$$

Where f_r is the shear strength of the screws between the frame and the lining and λ is a factor dependent on the geometrical properties of the wall and horizontal and vertical screw spacing. λ is given by (2).

$$\lambda = \sqrt{(L/n_h)^2 + (H/n_v)^2} \quad (2)$$

Where L is the length of the wall, H is the height of the wall, n_h is the number of screws in the top or bottom horizontal boundaries of the partition wall, and n_v is the number of screws in the left or right vertical boundaries of the partition wall.

Again, the total lateral displacement Δ_t in a partition wall, comprises of the following [16]:

- Flexural displacement of the frame $\Delta_f = \frac{PH^3}{3EAL^2}$, where P is the lateral force acting on the partition wall (it is assumed that the loads are uniformly distributed on both sides of the wall), and E and A are the modulus of elasticity and area of the timber chord, respectively.

- Shear displacement of the plasterboard lining $\Delta_s = \frac{PH}{GLt}$, where G and t are the shear modulus ($\approx$ 830 MPa ([17]) and thickness of the plasterboard lining, respectively.

- Screw-slip due to slippage of screws between the plasterboard lining and the frame $\Delta_{ss} = \frac{2d_{so}P}{n_h f_r}(1 + H/L)$, where d_{so} is the displacement at which the shear strength of the frame-to-plasterboard lining screws is reached. The values of d_{so} can be derived from screw-slip curves for connections between various plasterboards linings and internal frames. For example, the literature reports d_{so} = 1 mm for connections between gypsum plasterboard and timber frames [11], [18] and d_{so} =10 mm for connections between type X gypsum plasterboard lining and steel frame. And,

- The displacement of the whole wall due to racking caused by uplifting of bases $\Delta_{rk} = \frac{v_1 - v_2}{L_{12}}$, where v_1 and v_2 are the vertical uplifts of the wall, respectively, at points 1 and 2 (located in the plane of the wall), and L_{12} is the horizontal distance between points 1 and 2.

Δ_t is given by (5).

$$\Delta_t = \Delta_f + \Delta_s + \Delta_{ss} + \Delta_{rk} \quad (5)$$

Since plasterboard linings and plasterboard lining-to-frame screws are the primary contributors to wall stiffness [12], the equivalent lateral stiffness of a partition wall, K_{eq}, accounting for only the shear deformation of the plasterboard lining and the screw-slip mechanism, is given by (6) [15].

$$K_{eq} = \frac{L^2}{\frac{HL}{2Gt} + \frac{2d_{so}(HL+L^2)}{n_h f r}} \quad (6)$$

Some limitations of these theoretical formulations include:

- The shear strength calculated using (1) may be unreliable for partition walls, as it only considers the shear strength of lining-to-timber screw connections. Experimental results indicate that partition wall performance is influenced by multiple factors, such as screw (and/or adhesive) type, size, and spacing, lining type and thickness, material properties, hold-down details, and joint finish type [9], [10], [19]-[23].

- Equation (5) does not account for the additional drift allowance caused by the out-of-plane buckling of the linings [14]

- With the introduction of low-damage wall designs incorporating seismic reliefs or gaps [24]-[27], (5) requires modifications to incorporate this additional drift allowance.

This study reviews experimental tests and theoretical analyses of plasterboard-lined partition walls, assessing their initial stiffness, shear strength, and damage onset under lateral drift. Current theoretical formulations are refined to address identified shortcomings. Additionally, a Y-shaped, plasterboard-lined, timber-framed partition wall, representative of commercial buildings in New Zealand, was tested under quasi-static cyclic drifts to evaluate its bi-directional seismic performance, identify damage thresholds, and validate the refined theoretical predictions.

2 –PREDICTION OF ONSET DRIFTS FOR PARTITION WALL DAMAGE

This section outlines the shortcomings of the earlier discussed formulations and analysis methods in detail. Where possible and appropriate, these formulations have been revised in light of published research. Additionally, they are employed to estimate the response and damage thresholds of different types of partition walls found in the literature.

2.1 SHEAR STRENGTH ANALYIS

Studies have shown that plasterboard lining-to-frame screws can maintain their load-carrying capacity even during bearing failure, resulting in an actual shear strength that is 1.3 times higher than that predicted by (1) (overstrength) [28]. Experimental results indicate that the shear strength f_r of gypsum plasterboard lining – to – timber screws (gauge numbers 6, 8, and 10) is approximately 0.5 kN for single-layer of 10–12 mm linings [9], [11], [18], [28], [29] and 0.66 kN for double-layer linings [29]. However, factors such as overdriven screws and saturated or soaked plasterboard lining can significantly reduce the shear strength f_r by a factor of 1.3 and 4, respectively, often negating the overstrength [30].

To generalize the shear strength of partition walls, modification factors are introduced into (1) to account for different wall systems, plasterboard lining-to-frame connections, and joint finishes, leading to:

$$V_{ult} = \phi_f \phi_{sys} \phi_{con} \left(\frac{2f_r}{\lambda}\right) = \frac{2\psi f_r}{\lambda} \tag{7}$$

$$\Rightarrow P_{ult} = V_{ult} L = \frac{2\psi f_r L}{\lambda} \tag{8}$$

Where P_{ult} and V_{ult} are the ultimate shear strength and ultimate shear strength per unit length of the wall, respectively, and $\psi = \phi_f \phi_{sys} \phi_{con}$. ϕ_f, ϕ_{sys} and ϕ_{con} are factors related to the type of finishing in the joints, the type of partition wall system, and the type of gypsum plasterboard lining-to-frame connection, respectively.

The approximate values of these modification factors are determined directly from experimental results by comparing the ultimate shear strengths of similar partition wall configurations with varying details available in the literature. For example, ϕ_{sys} for partitions with return walls is taken as 2.0, based on experimental results from [23]. ϕ_{sys} for partitions with steel framing is calculated as 0.88, derived by dividing the ultimate strength of a steel-framed wall by that of a wood-framed wall with similar details, as reported in Table 3 of [11], i.e., $\phi_{sys} = 11.7/13.2 = 0.88$. These values are shown in Table 1.

2.2 DISPLACEMENT ANALYSIS

A lateral displacement equal to the cumulative vertical joint gap width Δ_{vgap} between linings and structural boundary elements can be accommodated before the linings and their connections fully engage to provide additional lateral stiffness in walls. Some partition walls systems [24]-[27] include vertical joint gaps along the intermediate or boundary joints of the walls for a low-damage performance.

Table 1: Approximate values of ϕ factors

ϕ_{sys}		
Source	**Type of rigid wall system**	ϕ_{sys}
---	Timber frame without return walls (Isolated / Planar Wall)	1.0
[23]	With return walls	2.0
[11]	Steel frame	0.88
[12]	Steel frame with the vertical slotted top track	0.65
ϕ_{con}		
Source	**Type of connection**	ϕ_{con}
---	Screws only	1.0
[21], [31]	Screw or nail and construction adhesive	1.6
ϕ_f		
Source	**Type of connection**	ϕ_f
---	Unfinished joint	1.0
[32]	Mesh joint tape and joint compound	1.5

In walls with friction-sliding frame connections that incorporate some horizontal joint gaps, a significant rocking displacement may occur due to the rocking of steel studs and plasterboard lining. Horizontal gaps can exist between the plasterboard linings or between frames and structural elements, allowing the wall to uplift without adding lateral strength or stiffness until the total horizontal joint gap width Δ_{hgap} is exhausted. In such cases, the top lateral displacement due to rocking of the wall is denoted as Δ_R which can be calculated using (9).

$$\Delta_R = \left(\frac{\Delta_{hgap}}{L}\right) \times H \tag{9}$$

For displacement demands less than Δ_{vgap} and Δ_R, the stiffness of such partition wall systems with vertical or horizontal gaps can be considered negligible.

Equation (9) does not account for the displacement caused by potential buckling of the end studs in steel-framed partition walls, a phenomenon observed in multiple tests [12], [32]. According to [12], studs are significantly weaker than other wall components, often leading to a high frequency of screw damage in steel-framed walls.

Additionally, when opposite corners of the plasterboard align with adjacent corners of the structural frame (or boundary elements) at the end of their rocking motion, the plasterboard lining experiences diagonal compressive forces. At this stage, the engaged corners are prone to crushing due to concentrated loads and impacts and subsequently the plasterboard lining tends to buckle in the out-of-plane direction. This out-of-plane buckling resembles the behaviour observed in glazed windows [33]. The Δ_s in (5) does not account for this buckling mechanism, as it assumes that plasterboards possess

https://doi.org/10.52202/080513-0688

sufficient stiffness to prevent out-of-plane deformation. However, this assumption may hold only when screws are used in conjunction with adhesives, which often leads to a more brittle failure mode [34].

The diagonal shortening of the plasterboard continues until it fails at its flexural tensile strength, leading to diagonal buckling failure. The corresponding lateral drift θ_{bk} associated with the lateral displacement Δ_{bk} due to this mechanism is approximated by (10) [33].

$$\theta_{bk} = \frac{1}{bh}\left(\frac{\sigma_f d^2}{\pi E t}\right)^2 \qquad (10)$$

Where b is the length of the wall or each plasterboard when the plaster-joint between the plasterboards is assumed to remain intact or damaged before buckling, respectively, h is the height of the wall (assuming that the plasterboard linings are same height as the walls), and d is the diagonal length of the wall $\left(d = \sqrt{b^2 + h^2}\right)$. Moreover σ_f, E and t are the modulus of rigidity or flexural strength (≈4 MPa [17], [35]), elastic modulus (≈2000 MPa [17], [35]), and thickness of gypsum plasterboard, respectively. Incorporating these different displacement components in (5) gives a general equation for the total displacement given by (11). The value of E varies widely due to several factors, including the type, thickness, density, and orientation of the gypsum plasterboard lining, the paper type used to encase the gypsum core, relative humidity, and the amount of handling before testing[17]. As a result, estimating the out-of-plane buckling load for plasterboard linings under specific site conditions remains challenging and unreliable.

$$\Delta_t = \Delta_f + \Delta_s + \Delta_{ss} + \Delta_{rk} + \Delta_R + \Delta_{vgap} + \Delta_{bk} \qquad (11)$$

Initially, the displacement components corresponding to the flexural deformation of the internal frame, racking behaviour, rocking due to horizontal and vertical seismic reliefs, and buckling of plasterboard can be considered negligible (i.e., Δ_f, Δ_{rk}, Δ_R, Δ_{vgap} and $\Delta_{bk} \to 0$) in rigid partition walls with adequate hold-down capacity. Thus, (11) is simplified as shown in (12).

$$\Delta_t = \Delta_s + \Delta_{ss} = \left[\frac{H}{GLt} + \frac{2d_{so}}{n_h f_r}(1 + H/L)\right]P \qquad (12)$$

An example of the predicted load vs. displacement $(\Delta_s + \Delta_{ss})$ curves using (12) is plotted in Fig. 2 for a wall specimen tested by [36]. The parameters considered here are $d_{so} = 3mm$ and $f_r = 1226N$ [36]. Additional comparisons can be found in [14]

Fig. 2 shows that the line connecting the origin with the ultimate displacement given by (12) provides a reasonable estimate of the equivalent elastic stiffness. However, (12) underestimates the racking displacements at higher load levels in all cases. As a result, (12) cannot be relied upon to predict the lateral in-plane response of partition walls accurately [14].

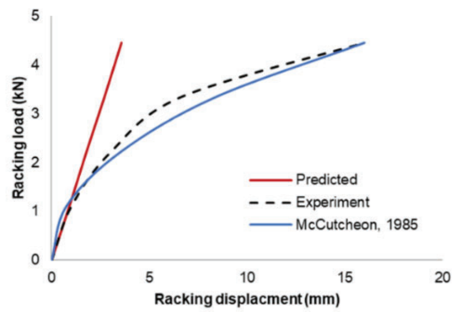

Figure 2. Load-displacement curves for wall: 8 ft (2440 mm) by 7.87 ft (2400 mm) wall with 8 in (203mm) screw spacing, two 4 ft (1220 mm) long linings [36]

Given the ultimate strength P_{ult} and initial stiffness K_{eq} of a partition wall, determined by (8) and (6), respectively, the inter-storey drift at which the ultimate strength is achieved, θ_{ult}, can be calculated as given by (13).

$$\theta_{ult} = \frac{P_{ult}}{K_{eq} H} \qquad (13)$$

Similarly, the onset drifts for the screw damage θ_{fr} can be approximated as given by (14).

$$\theta_{fr} = \frac{V_{fr} L}{K_{eq} H} \qquad (14)$$

The accuracy of (14) in predicting the onset drift for screw failure is assessed by comparing with the experimental drifts when screw failures were observed for different types of rigid partition walls, available in the literature, as shown in Table 2. In Table 2, it can be observed that the theoretically approximated and experimentally observed values are in a reasonable agreement. The probable reason for some variations may be the property of the setting applied over the screw head to conceal the damage to the screws [32], screws being overdriven [17] or the selection of the values of d_{so} and f_r.

Table 2: Comparison between theoretical on-set and experimental observed drifts for screw-failure

Source	Frame type	Onset inter-story drift (%)	
		Theoretical	Experimental
[25]	Timber	0.21	0.30
[37]	Timber	0.19	0.30
[13]	Steel	1.00	0.78
[26]	Steel	1.17	0.96

2.3 BILINEAR BACKBONE CURVE PREDICTION

Assuming symmetrical behaviour of a partition wall under lateral loads interconnecting the points: $A(-\theta_{bk}, 0)$, $B(-\theta_{ult}, -P_{ult})$, $C(0,0)$, $D(\theta_{ult}, P_{ult})$ and $E(\theta_{bk}, 0)$

https://doi.org/10.52202/080513-0688

form a bilinear backbone curve (see Fig. 3). Here, θ_{bk} represents the extreme damage state at which the partition wall's capacity theoretically reaches zero. The segments BA and DE are represented as lines with a negative slope, reflecting the progressive damage occurring at increasing drift levels. This approach avoids modelling a sudden drop to zero at points A and E, when θ_{bk} is reached. An example of the predicted and experimental backbone curves (redrawn as bilinear curves) a partition wall reported in the literature [13] is shown in Fig. 3. Addition comparisons can be found in [14]. The comparison indicates that the predicted curves can reasonably approximate the experimental bilinear backbone curves.

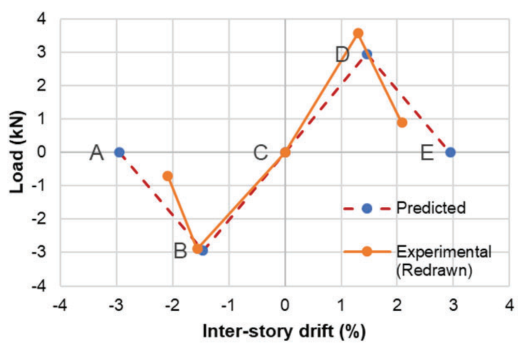

Figure 3. Comparison between predicted and experimental backbone curves (redrawn as bilinear curves): Specimen NDS from [13]

In reality, some residual capacity remains at the buckling drift θ_{bk}. The residual capacity is not captured by the simplified prediction model used here. Despite this, the predicted buckling drift (corresponding to zero capacity) is typically higher than the experimentally measured buckling drift, reducing the impact of ignoring residual capacity in the post-peak response until the experimental buckling drift is reached. The predicted response beyond the experimental drift limit may not significant, as these drift levels exceed the maximum inter-storey drift expected at the ultimate limit state (e.g., 2.50% as per New Zealand standards [38]).

3 – CAPACITY BASED DESIGN FOR SCREW SPACING

In horizontally oriented plasterboard linings, the shear strength of the plastered joint between the plasterboard linings can be considered equivalent to the combined shear strengths of the screws located along both sides of the joint in the wall, as illustrated in Fig. 4. For one of the plasterboards,

$$\frac{P_{ps}}{2} = \left(\frac{L}{X_{ss}}\right) f_r \tag{15}$$

Where L is the length of the wall, f_r is the shear-strength of each screw connection between the plasterboard lining-and-internal stud, and X_{ss} is the screw spacing along each side of the plastered joint (or equal to the spacing of the studs when screws are driven only to the studs).

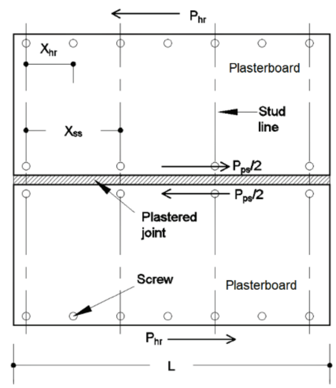

Figure 4. Schematic diagram of force transfer mechanism through plastered joint in horizontally oriented plasterboards [14]

The shear strength of the plastered joint P_{ps} is given by $P_{ps} = p_s R_p$, where p_s and R_p are the shear strength per unit length (shown in Table 3) and the total length of the plastered joint, respectively. For horizontal joints along the length of the wall, R_p can be taken equal to the length of the wall L. Substituting these in (15) gives,

$$\frac{p_s L}{2} = \left(\frac{L}{X_{ss}}\right) f_r \tag{16}$$

$$\Rightarrow X_{ss} = \frac{2f_r}{p_s} \tag{17}$$

For a standard case with $f_r = 0.5kN$, and $p_s = 2.5kN/m$, we obtain $X_{ss} = 400mm$. Generally, at the boundaries, the spacing of the screws (X_{hr}) is kept smaller than that in the field region i.e., $X_{hr} < X_{ss}$.

Table 3: Shear strength of typical plastered joints

Type of joint	p_s (kN/m)
Perforated paper-tape with three coats of cement joint [9], [16]	7.2 to 8.0
Fibreglass tape joint [9]	5.9
Paper-tape filled with two coats of bedding compound [35]	2.0 to 2.5*
Back-blocked joint (a strip of gypsum plasterboard adhered behind the joint using GIB® Cove adhesive) [35]	3.0 to 4.0*

**These values are indicative only.*

Similarly, if the plasterboards are oriented vertically then,

$$X_{vr} = \frac{2f_r}{p_s} \tag{18}$$

If the vertical joints are provided along the stud line, it is easier to space the vertical screws required by (18) along both sides of the joint. The cracking of the plastered joint before the screw failures may be desirable as the repair process for plaster cracks may be easy and economical. Therefore, it may be prudent to conservatively provide

https://doi.org/10.52202/080513-0688

screw spacing taken equal to or less than X_{vr} along the boundaries.

4 – EXPERIMENTAL TEST

4.1 BARE FRAME SETUP, LOADING PROTOCOL

The test frame, shown in Fig. 5, was designed with hinged connections at the beam-column joints and at the column bases, allowing for a shear mode of deformation when subjected to lateral cyclic displacements at the top of the frame. The top and bottom of the frame were connected to 120 mm thick reinforced concrete slabs, with a clear height of 2405 mm between them. Additional details on the test frame setup can be found in [39], [40]. A 200 kN actuator, supported by a reaction frame, was bolted to the centre of the ceiling slab to apply lateral loading. The load applied to the specimen was measured using a 50 kN load cell with an accuracy of ±3 N.

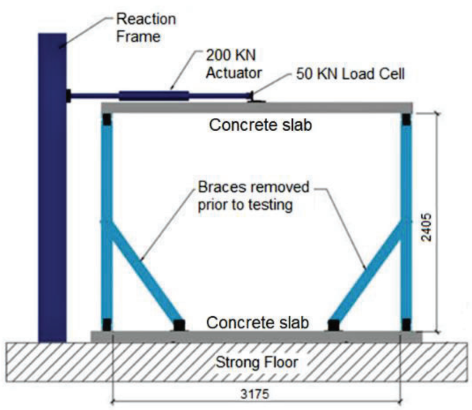

Figure 5. Steel-frame structure-elevation [39]

The loading protocol consisted of a displacement-controlled unidirectional quasi-static cyclic drifts as defined in FEMA-461[41], with the loading sequence illustrated in Fig. 6.

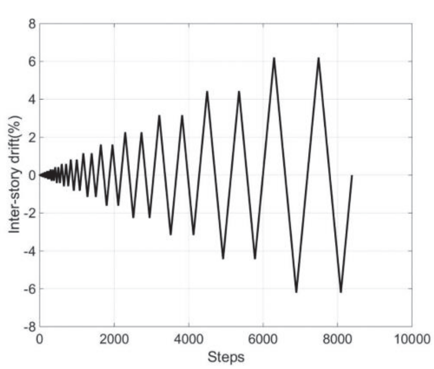

Figure 6. FEMA-461 loading protocol [41]

Two cycles were applied at each drift amplitude, with each step's drift amplitude set to 1.4 times that of the preceding step. A total of 16 drift steps were applied, reaching a maximum drift of 6.21% in the frame axis which is more than twice the allowable ultimate limit state of 2.50%. The response of the bare frame was found to be approximately linear, exhibiting a stiffness of 10.1 N/mm [14].

4.2. TIMBER-FRAMED PARTITION WALL SPECIMEN DETAILS

A rigid timber-framed wall (TFW) specimen with details commonly used to construct interior partition walls in New Zealand buildings was constructed between two parallel concrete slabs supported by steel frames shown in Fig. 5. The TFW specimen was oriented oblique to the loading direction and had multiple short wing-walls with one 'L'-junction (in the west) and one Y-junction (in the east), as shown in Fig.7. It enabled examination of the bi-directional performance of walls under a unidirectional quasi-static cyclic loading. Moreover, assessment of the performance of walls with multiple orientations and junctions in a single test was possible.

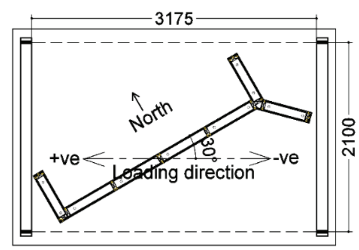

Figure 7. Steel-frame structure with 'y' shaped TFW specimen-plan [14]

The specimen consisted of three types of 116 mm thick and 2.405 m high walls: (1) Planar Wall inclined 30°, (2) Return Wall inclined 60° and (3) Inclined Wall inclined 15° to the loading direction as shown in Fig. 8.

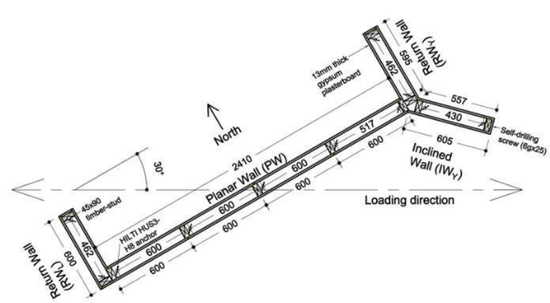

Figure 8. Details of TFW specimen-plan [14]

The TFW specimen was assembled with horizontal timber runners (90 mm x 45 mm) fastened to the concrete slabs (ceiling and floor slabs) using HILTI® HUS3 - H8 anchor bolts, spaced as shown in Fig. 5c. Timber studs of the same

https://doi.org/10.52202/080513-0688

dimensions were then attached to these runners at a regular spacing of 600 mm c/c by driving three nails at an angle, with two from one side and one from the other. The vertical joint at the south of the Y-junction was reinforced with 135° 0.55BMT galvanized steel angles screwed to the studs. A single layer of 13 mm thick gypsum plasterboard lining was attached to both sides of the studs and runners using GIB® Grabber self-tapping drill point screws (6g x 25 mm), with screw spacing maintained at 300 mm c/c along the boundaries and within the field of the partition wall. The joints were then plastered with two coats of GIB® Tradeset 90-minute premium jointing compound, accompanied by jointing tape and internal or external corner beads (/L-trims) where necessary. A final coat of plaster was applied using GIB® Trade Finish, after which the surface was sanded and finished with two coats of paint before testing.

4.3 INSTRUMENTATION

The TFW specimen was equipped with linear potentiometers to measure vertical and out-of-plane displacements. These potentiometers recorded the relative linear displacement between the points where they were attached to the TFW specimen and the surface of the concrete slab. The visual inspection of the specimen was done after each step of the applied loading protocol (Fig. 6) and any damage observed was photographed and manually recorded.

4.4 OBSERVED DAMAGE

The observed damage to the TFW specimen during the experiment is shown in Fig. 9 and summarized below.

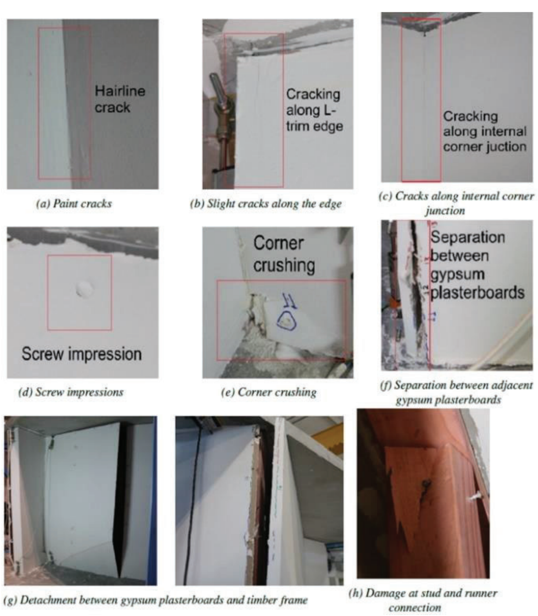

(a) Paint cracks (b) Slight cracks along the edge (c) Cracks along internal corner junction
(d) Screw impressions (e) Corner crushing (f) Separation between adjacent gypsum plasterboards
(g) Detachment between gypsum plasterboards and timber frame (h) Damage at stud and runner connection

Figure 9. Examples of observed damage to the tested TFW specimen [14]

- The first hairline crack was observed early in the test at an inter-story drift of 0.09%, forming between the Planar Wall and the intersecting walls.
- Cracks in the plasterboard linings initially appeared around the periphery of corner beads, with new cracks branching off from these locations (see Fig. 9b).
- Screw impressions became visible through the finished compound over the screw heads, along the top and bottom boundaries of the plasterboard lining, appearing after 0.51% inter-story drift cycles corresponding to the Planar Wall (see Fig. 9d).
- The ripping of joint tapes and the widening of cracks along the corner beads (Fig. 9f and Fig. 9g) signalled relative movement between adjacent plasterboard linings.
- The plasterboard linings buckled diagonally in the out-of-plane direction and eventually detached from the timber frame (see Fig. 9g).
- The timber-frame was concealed behind the gypsum plasterboards, the exact drift at which the frame was damaged was not possible to be determined. At the end of the tests, the timber frame was observed to sustain only minor damage at the stud and runner joints (see Fig. 9h), even after a high in-plane drift of 5.38% corresponding to the Planar Wall.

Comprehensive details on the damage progression in the TFW specimen is available in [14].

4.5 EXPERIMENTAL RESULTS AND THEORETICAL PREDICTIONS FOR DAMAGE THRESHOLD

The maximum shear force, initial stiffness, expected drifts for screw damage, and gypsum plasterboard lining buckling for the TFW specimen were calculated using (8), (6), (14) and (10), respectively. These calculations incorporated the modification factors and parameters listed in Table 4. The theoretical predictions were then compared with the experimental results, as shown in Table 5. The comparison indicates that the theoretical values are in reasonable agreement with the experimental findings. However, the stiffness of the walls was underestimated, which is likely due to the neglect of the three-dimensional nature of the wall specimen in the stiffness estimation process.

Table 4: Values of the parameters for the tested specimen

$X_h = 300mm$	$\phi_f = 1.50$	$\lambda = 377.25$
$X_v = 300mm$	$f_r = 0.50kN$	$L = 2410mm$
$d_{so} = 1mm$	$\phi_{sys} = 2.00$	$H = 2405mm$
$\phi_{con} = 1.00$	$p_s = 2.50kN/m$	

https://doi.org/10.52202/080513-0688

Table 5: Comparison between experimental results and theoretical predictions for TFW specimen

Parameter	Theoretically predicted	Experimentally obtained	Percentage difference
Ultimate Shear strength per unit length of the wall (V_{ult})	$7.95 kN/m$	$24.80\ kN\ /3.271\ m\ =\ 7.58\ kN/m$	4.88%
Ultimate shear strength (P_{ult})	$7.95 \times 3.271 = 26kN$	$24.08kN$	4.88%
Equivalent lateral stiffness(K_{eq})	$0.93kN/mm$	$1.72kN/mm$ (At 75% of the ultimate load)	45.9%
Screw spacing (X_{vr})	$400mm$	$300mm$	33.33%
Screw failure onset drift (θ_{fr})	0.40%	0.51%	21.57%
Plasterboard buckling drift (θ_{bk})	5.53%	5.38%	2.78%

4.6 FORCE-DISPLACEMENT ENVELOPE

Since the original force-drift data obtained from the experiment was noisy, the moving average for each force value was taken (with window size 3, which incorporated one value before and after the considered value) to smoothen the curve. The resulting force-drift hysteretic loops are shown in Fig. 10. Fig. 10 also shows the loading stage corresponding to the onset of different damage observed during the test as the load-displacement envelope curve in the linear elastic region is predicted by interconnecting the points: $A(-\theta_{bk}, 0)$, $B(-\theta_{ult}, -P_{ult})$, $C(0,0)$, $D(\theta_{ult}, P_{ult})$ and $E(\theta_{bk}, 0)$for this specimen.

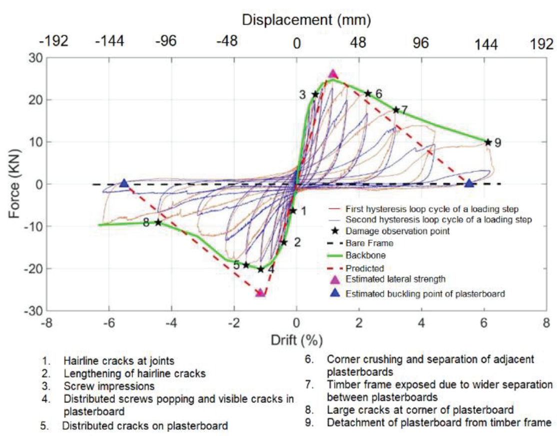

Figure 10. Hysteresis loop with damage points in the specimen [14]

The initial stiffness of the partition wall is primarily provided by the plasterboard, stopped joints, and the screw connections between the plasterboards and the internal timber frame. During the unloading phase at the peak of each cycle, the applied force rapidly dropped close to zero, followed by a gradual reduction in displacement with minimal force change. With each successive loading cycle, the specimen softened due to the progressive reduction in stiffness, a trend that became more pronounced after the failure of screws.

Significant strength degradation was observed once the ultimate strength of the wall was reached, consistent with the typical behaviour of rigid framed partition walls reported in other studies [13], [32].

As shown in Fig. 10, the predicted point of screw failure closely aligns with the earliest observed screw failures (or impressions) in the experiment, suggesting that (8) provides a reasonable estimate for the onset drift of screw failures. At the buckling θ_{bk}, the experimental curve still retained some residual load, whereas the predicted curve neglected this residual capacity. Elaborate behaviour of the tested TFW specimen is available in [14].

5 – CONCLUSIONS

This paper presents the results of a theoretical and experimental study on the seismic performance of an interior timber-framed partition wall, constructed using details commonly found in New Zealand commercial buildings and subjected to unidirectional quasi-static cyclic loading. The oblique orientation of the specimen allowed for an assessment of the bi-directional performance of the partitions.

Theoretical equations, either derived from linear elastic analyses or proposed in published literature for estimating the strength, stiffness, displacements, and various damage states of plasterboard partition walls, were evaluated and modified based on recent research. Additionally, theoretical expressions were developed to determine the necessary horizontal and vertical screw spacing to prevent screw failures before damage occurs at the plastered joint between plasterboards during an earthquake.

A Y-shaped timber-framed partition wall specimen was tested to determine the drift limits at which varying levels of damage occur and to validate the accuracy of the theoretical formulations. The screw failures and corner crushing of plasterboard linings was observed in the tested specimen at inter-storey drifts of 0.51% and 1.40%, respectively. The theoretical estimates for the drift at which the wall reached its shear strength and the point at which the plasterboard experienced diagonal buckling failure were found to be in reasonable agreement with the experimental results.

6 –ACKNOWLEDGEMENTS

The work presented in this paper has been partly funded by the International Collaborative Research program of the Disaster Prevention Research Institute, Kyoto University under Project Number 28W-03 (PI: Timothy Sullivan), the NZ Property Council, and Quake Centre. This project was fully supported by QuakeCoRE, a New Zealand Tertiary

Education Commission-funded Centre. This is QuakeCoRE publication number **1031**. Gratitude is expressed to industry partner Winstone Wallboards Ltd. for their professional support. Special thanks are due to all the technical staff for their assistance and support at the University of Canterbury Laboratories.

8 –REFERENCES

[1] A. Baird *et al*, "Seismic performance of vertical nonstructural components in the 22 February 2011 Christchurch earthquake," *Earthquake Spectra,* vol. 30, *(1),* pp. 401–425, 2014.

[2] M. Rosevear and M. D. Curtis, *Physical Characteristics of New Non-Residential Buildings 2015.* 2017.

[3] Standards Australia and Standards New Zealand, "AS/NZS 2558: Gypsum plasterboard," *Standards Australia / Standards New Zealand,* 2018.

[4] Standards Australia and Standards New Zealand, "AS/NZS2589: Gypsum linings-Application and finishing," *Standards Australia / Standards New Zealand,* 2017.

[5] D. P. Fischer, *Shake Table Tests of a Two-Story Woodframe House.* 2001.

[6] K. M. Mosalam, *Seismic Evaluation of an Asymmetric Three-Story Woodframe Building.* 2002.

[7] I. P. Christovasilis, A. Filiatrault and A. Wanitkorkul, *Seismic Testing of a Full-Scale Two-Story Light-Frame Wood Building: NEESWood Benchmark Test.* 2009.

[8] C. Ekiert and A. Filiatrault, "Fragility curves for wood light-frame structural systems," *Background Document FEMA P-58/BD-3.8,* vol. 1, 2008.

[9] B. Golledge, T. Clayton and G. Reardon, "Racking performance of plasterboard-clad steel stud walls," 1992. Available: https://scholarsmine.mst.edu/cgi/viewcontent.cgi?article=1794&context=isccss.

[10] T. S. Tarpy Jr, "Shear resistance of steel stud wall panels: a summary report," 1984.

[11] S. Swensen, G. G. Deierlein and E. Miranda, "Behavior of screw and adhesive connections to gypsum wallboard in wood and cold-formed steel-framed wallettes," *J. Struct. Eng.,* vol. 142, *(4),* pp. E4015002, 2016.

[12] J. I. Restrepo and A. M. Bersofsky, "Performance characteristics of light gage steel stud partition walls," *Thin-Walled Structures,* vol. 49, *(2),* pp. 317–324, 2011.

[13] S. Amer, S. Hamoush and T. Abu-Lebdeh, "In-plane performance of gypsum board partition wall systems subjected to cyclic loadings," *Journal of Constructional Steel Research,* vol. 124, pp. 23–36, 2016.

[14] J. Bhatta *et al*, "Theoretical and experimental evaluation of timber-framed partitions under lateral drift," *Bulletin of the New Zealand Society for Earthquake Engineering,* vol. 54, *(4),* pp. 263–281, 2021.

[15] S. Nie *et al*, "Investigation on the Design Method of Shear Strength and Lateral Stiffness of the Cold-Formed Steel Shear Wall," *Mathematical Problems in Engineering,* vol. 2020, *(1),* pp. 8959712, 2020.

[16] S. J. Thurston, *Report on Racking Resistance of Long Sheathed Timber Framed Walls with Openings.* 1993.

[17] GA-235-2019, "Gypsum board typical mechanical and physical properties," Gypsum Association, 2019Available: https://www.americangypsum.com/sites/default/files/documents/GA-235%20Gypsum%20Board%20Typical%20Mechanical%20and%20Physical%20Properties.pdf.

[18] A. Liu and R. H. Shelton, *Seismic Effects of Structural Irregularity of Light Timber-Framed Buildings.* 2018.

[19] K. Gatto and C. Uang, *Cyclic Response of Woodframe Shearwalls: Loading Protocol and Rate of Loading Effects.* 2002.

[20] K. M. McMullin and D. Merrick, *Seismic Performance of Gypsum Walls: Experimental Test Program.* 2002.

[21] M. G. Oliva, *Racking Behavior of Wood-Frame Gypsum Panels Under Dynamic Load.* 1990.

[22] R. W. Wolfe, *Contribution of Gypsum Wall Board to Racking Resistance of Light-Frame Walls.* 1983*439*.

[23] Y. L. Liew, C. Duffield and E. Gad, "The influence of plasterboard clad walls on the structural behaviour of low rise residential buildings," *Electronic Journal of Structural Engineering,* vol. 2, pp. 1–16, 2002. .

[24] AWCI, "Code of practice for the seismic design and installation of non-structural internal walls and partitions," 2018Available: https://awci.org.nz/wp-

 https://doi.org/10.52202/080513-0688

content/uploads/COP-Internal-Walls-and-Partitions-coloured.pdf.

[25] A. S. Tasligedik, "Damage mitigation strategies for non-structural infill walls." 2014. Available: https://ir.canterbury.ac.nz/bitstream/handle/10092/9462/thesis_fulltext.pdf?sequence=1&isAllowed=y.

[26] T. Pali *et al*, "In-plane quasi-static cyclic tests of nonstructural lightweight steel drywall partitions for seismic performance evaluation," *Earthquake Eng. Struct. Dyn.,* vol. 47, *(6),* pp. 1566–1588, 2018.

[27] G. Magliulo *et al*, "Seismic performance evaluation of plasterboard partitions via shake table tests," *Bulletin of Earthquake Engineering,* vol. 12, pp. 1657–1677, 2014.

[28] I. Filomena, L. F. Jia and B. Yu, "Capacity of screw connections between plasterboard panels and cold-formed steel for modular buildings," in 2018.

[29] W. Chen, J. Ye and T. Chen, "Design of cold-formed steel screw connections with gypsum sheathing at ambient and elevated temperatures," *Applied Sciences,* vol. 6, *(9),* pp. 248, 2016.

[30] L. C. Vieira Jr and B. W. Schafer, "Lateral stiffness and strength of sheathing braced cold-formed steel stud walls," *Eng. Struct.,* vol. 37, pp. 205–213, 2012.

[31] A. Filiatrault and R. O. Foschi, "Static and dynamic tests of timber shear walls fastened with nails and wood adhesive," *Canadian Journal of Civil Engineering,* vol. 18, *(5),* pp. 749–755, 1991.

[32] A. M. Memari *et al*, "Lateral load resistance evaluation of wood-and steel-stud partition shear walls," *J. Archit. Eng.,* vol. 15, *(4),* pp. 122–130, 2009.

[33] H. Sucuoğlu and C. G. Vallabhan, "Behaviour of window glass panels during earthquakes," *Eng. Struct.,* vol. 19, *(8),* pp. 685–694, 1997.

[34] D. J. Dowrick and P. C. Smith, "Timber sheathed walls for wind and earthquake resistance," *Bulletin of the New Zealand Society for Earthquake Engineering,* vol. 19, *(2),* pp. 123–134, 1986.

[35] Winstone Wallboards, "Gib-site-guide," 2018.

[36] W. J. McCutcheon, "Racking deformations in wood shear walls," *J. Struct. Eng.,* vol. 111, *(2),* pp. 257–269, 1985.

[37] K. M. McMullin and D. S. Merrick, "Seismic damage thresholds for gypsum wallboard partition walls," *J. Archit. Eng.,* vol. 13, *(1),* pp. 22–29, 2007.

[38] New Zealand Standard, "NZS 1170.5:2004, Structural Design Actions Part 5: Earthquake actions," 2004.

[39] J. Mulligan, T. Sullivan and R. Dhakal, "Experimental study of the seismic performance of plasterboard partition walls with seismic gaps," *Bulletin of the New Zealand Society for Earthquake Engineering,* vol. 53, *(4),* pp. 175–188, 2020.

[40] J. Mulligan, T. J. Sullivan and R. P. Dhakal, "Experimental seismic performance of partly-sliding partition walls," *J. Earthquake Eng.,* vol. 26, *(3),* pp. 1630–1655, 2022.

[41] FEMA, *Interim Testing Protocols for Determining the Seismic Performance Characteristics of Structural and Nonstructural Components.* 2007.